Progress In Electromagnetics Research, Vol. 108, 205–219, 2010

ANALYSIS OF MICROWAVE EMISSION OF EXPONENTIALLY CORRELATED ROUGH SOIL SURFACES FROM 1.4 GHz TO 36.5 GHz

P. Xu † **and K.-S. Chen**

Communication Research Center
Center for Space and Remote Sensing
National Central University
Chung-Li 32054, Taiwan

L. Tsang

Department of Electrical Engineering
University of Washington
Seattle, WA 98195, USA

Abstract—We analyzed the microwave emission from a rough soil surface with exponential correlation by characterizing its dependences of polarization, look angle, and frequency. Using the same set of physical surface parameters of *rms* height and correlation lengths, results are obtained for a wide range of frequencies at 1.4 GHz, 5 GHz, 10 GHz, 18 GHz, and 36.5 GHz. Accurate simulations for the 2-D scattering problem are conducted by Galerkin's method with the rooftop basis function, followed by near-field integration, fine discretization, and cubic spline interpolation of surfaces. The multilevel UV method was employed to accelerate the solution. Accuracy is ensured by energy conservation check. Simulation results are compared with SPM, KA and AIEM. Results suggest that there exists distinct emission characteristic between the exponential and the Gaussian correlated surface. These characteristics should be very useful in developing retrieval algorithm of the soil moisture from emissivity measurements.

Received 27 July 2010, Accepted 10 September 2010, Scheduled 17 September 2010
Corresponding author: K.-S. Chen (dkschen@csrsr.ncu.edu.tw).
† Also with School of Electronic Information, Wuhan University, Wuhan 430079, China.

1. INTRODUCTION

Passive microwave remote sensing of land has been theoretically and experimentally studied for many years [1–12] and found in many practical applications, such as soil moisture estimation, ice and snow cover mapping from SSMI, AMSR-E sensors, etc. Understanding the characterization of microwave emissivity from rough surface is essential for better estimation of surface brightness temperature from microwave radiometers [5, 6, 10]. In modeling microwave emission from a bare surface, Gaussian correlation function is commonly used to describe the horizontal roughness scale. Inversion algorithm is then developed to retrieve the soil moisture, such as the Q-H approach by Wang et al. [3] and more advanced ones by others [9–12].

It is well known that surface spectrum form, or the correlation function, controls the angular behavior of the scattering coefficient [13–19]. Two limiting cases with distinct frequency decay rates are Gaussian and exponential correlation functions. The use of a Gaussian correlation function is not appropriate for land surfaces. Natural surfaces can have different types of correlation functions. There is also the presence of vegetation, rocks, etc. However, exponential correlations appear to match experimental data much better than Gaussian correlation functions [20, 21]. As will be illustrated in next section, Gaussian correlated surface has much fast decay rate than that of an exponential one. Therefore, it is important to explore the characteristics of from a rough soil surface with exponential correlation in terms of its dependences of polarization, look angle, and frequency, before a better a soil moisture retrieval algorithm for emissivity observation can be developed.

In active microwave remote sensing, the scattering mechanisms and properties have been extensively studied and understood in deeper insight [4, 5, 13, 19, 22]. In terms of numerical simulation and theoretical modeling, the accuracy requirement and error tolerance are somewhat looser because the scattering coefficient is usually measured on the order of few dBs. On the contrary, for passive microwave remote sensing, since we are dealing with the emissivity with value between 0 and 1, the high accuracy becomes critical. For example, merely a 1% emissivity error produces 3 K in brightness temperature (for 300 K physical temperature), barely acceptable in many applications. Recently, a fast, accurate, and reliable numerical simulation for 2D surface scattering problem was proposed, where both scattering and emission from exponentially correlated surface were reported [18]. The proposed simulation method offers a very powerful tool to better understand the role played by the surface

spectra in microwave emission that is difficult, if not impossible, ever before. We presented results over a wide range of frequency from 1.4 GHz to 36.5 GHz, using the same set of physical parameters of *rms* height and correlation lengths. Using a realistic *rms* height of 1 cm for soil surface, kh is 0.29 at 1.4 GHz and kh becomes 7.64 at 36.5 GHz, where k is the wavenumber and h is the *rms* height. It is essential to perform numerical simulations, as analytic theory usually is limited in applicability in the range of kh. We also made comparisons of simulations with SPM, KA and AIEM [16, 17]. In the next section, description of the numerical simulation of surface emissivity will be given. In all cases studied, wet soil surfaces with Gaussian and exponential correlation functions were considered for purpose of comparison. Results compared with known theoretical models were also illustrated. Section 3, the main body, focuses on detail discussions of emissivity from exponentially correlated surface by observing the frequency, polarization, and look angle dependences. The frequency correlation between L, C, X bands was simulated as well. The impacts on soil retrieval algorithm development were briefly outlined. Finally, conclusions were drawn.

2. NUMERICAL SIMULATIONS OF ROUGH SURFACE EMISSIVITY

In this study, numerical simulations were carried out to compute the emissivity from rough surfaces with both exponential and Gaussian correlation functions. For the purpose of this study, a 2D problem was considered. One of the critical issues to compute the emissivity is to guarantee the energy conservation. Less than 0.5% of error in energy conservation was generally required. This poses a great challenge for numerical simulations even for a 2D problem especially for the surface with exponential correlated due to fine structures. Accurate calculation of the surface currents requires a much higher sampling rate to digitize the surface and then solves the Maxwell's equations. This is equivalent to requiring much larger computation resources (computation time and memory storage). The numerical scheme that efficiently and effectively solves the Maxwell equations was proposed in [18]. To give a better idea, Fig. 1 illustrates the Gaussian and exponential surface spectra, $W(K)$, with correlation length of 4 units. It is clearly shown that the exponential correlated surface has much stronger high frequency components corresponding many fine structures of the surface profile, resulting fast fluctuations of the induced surface current when excited by the incident wave. On the other hand, Gaussian correlated surface contains much less

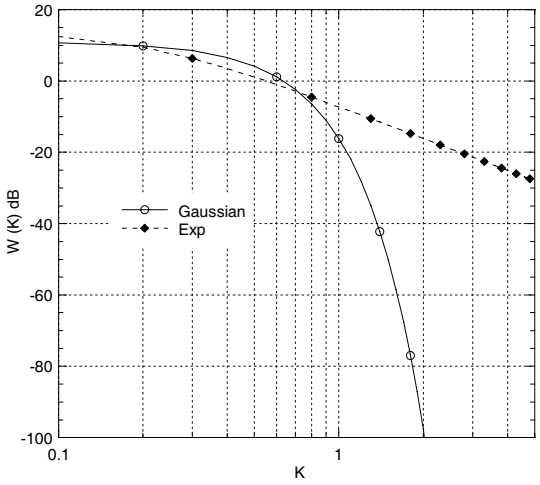

Figure 1. Surface spectra shows the difference of Gaussian and exponential correlated surface with correlation length of 4 units.

high frequency components as its spectra decays very fast as frequency increases. Hence, it is constructive to investigate the emissivity from Gaussian and exponential correlated surfaces.

When comes to numerical simulation, representation of such fine structures should be well devised so that depending on the wavelength the microwave can sense them all. Detailed steps of surface generation are referred to [18, 22]. As a result, as many as 1000 points per wavelength was used. As for numerical Maxwell model with 2-D simulations (NMM2D) for scattering and emission, we use the rooftop function and Galerkin's method with numerical integration of near-field impedance matrix elements. A dense discretization of a surface is used. Cubic spline interpolation (CSI) is employed to connect knots on random rough surface. Numerical accuracy convergence tests are performed for numerical solutions of Maxwell equations by varying the number of points from 13 to 103 points per wavelength in the dielectric medium, corresponding to 50–400 points per free wavelength. Since we discretize to as many as 400 points per free wavelength, the number of unknowns is more than 80 000 even for a 100-wavelength-long surface. NMM2D simulations are accelerated by the multilevel UV method of matrix solver [23, 24]. The relative permittivities of wet soil for a silt loam with sand of 17.16%, silt of 63.84%, clay of 19.00%, and temperature of 23°C for moisture content of 30.6% at frequency bands of 1.4 GHz, 5 GHz, 10 GHz, 18 GHz, and 36.5 GHz are listed in Table 1 [25]. Note that value at 36.5 GHz was obtained by extrapolation.

Table 1. The relative permittivities of wet soil of 30.6% moisture content.

Frequency (GHz)		1.4	5	10	18	36.5
$\varepsilon' + j\varepsilon''$	ε'	15.22	15.57	14.15	10.85	8.0
	ε''	3.45	3.71	5.21	6.13	7.5

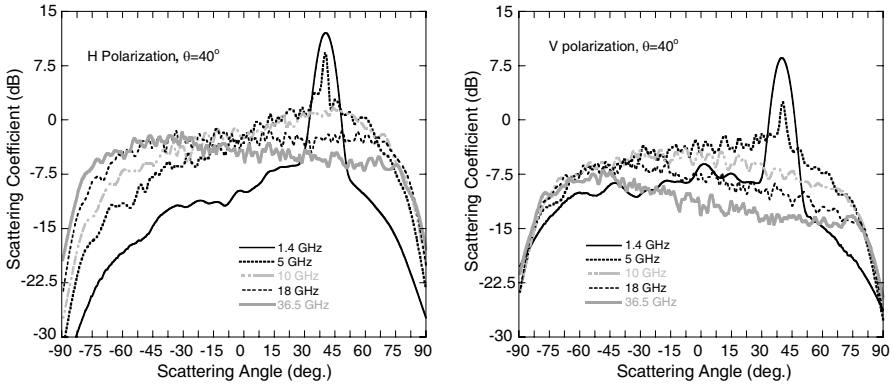

Figure 2. Bistatic scattering coefficients with $h = 1\,\text{cm}$, $l = 6\,\text{cm}$, $\theta_i = 40^\circ$ at 1.4 GHz, 5 GHz, 10 GHz, 18 GHz, and 36.5 GHz.

Figure 2 illustrates the bistatic scattering coefficients at frequency of 1.4 GHz, 5 GHz, 10 GHz, 18 GHz, and 36.5 GHz for look angle of 40° with surface *rms* height, h and correlation length, l, of 1 cm and 6 cm, respectively. It should be mentioned that results given here were averaged over 40, 40, 50, 60, 60 realizations, respectively at 1.4 to 36.5 GHz; at higher frequencies, more averages are needed to get smoother curve. At both H and V polarizations, strong returns at forward direction were observed for lower frequencies of 1.4 GHz and 5 GHz. When frequency increases, strong peaks at forward direction begin to disappear and flatten, and eventually is weaker than those at backward direction. The forward scattering decays faster at V-polarized than that at H-polarized. Overall, the H-polarized has stronger scattering returns and higher dynamic range than the V-polarized, as is well-known and can be attributed to stronger multiple scattering for H polarization.

Figure 3 shows a comparison of bistatic scattering coefficients at 36.5 GHz between the simulation (NMM2D) and the second-order small perturbation model (SPM2) [22, 26] with $h = 2\,\text{cm}$, $l = 12\,\text{cm}$, $\theta = 40^\circ$ for both H and V polarizations. It can be seen from the

bistatic scattering that the angular trend is quite flat partially because the surface is very rough ($kh = 15.289$, $kl = 91.734$). The polarization difference remains quite equable as scattering angle changes, except near grazing. Under this case, the backscattering is large than the forward scattering at both polarizations. This is, however, not ever seen for a Gaussian surface. The reason maybe due to the lack of contributions from the fine scale structures, as can be revealed from its spectra in Fig. 1. The comparison also indicates that the angular trend predicted by SPM2 is totally unacceptable. Due to very large surface roughness, the series in Kirchhoff approximation (KA) and AIEM fail to converge without considering the multiple scattering effects. Thus the results of KA and AIEM are not shown in this figure. Further comparison of emissivity computed by NMM2D and SPM2 was also made, where NMM2D reports the emissivity of 0.889 and 0.965, while SPM2 predicts the emissivity of 3.142 and 4.094 for H-polarized and V-polarized, respectively, again implying inapplicable of the SPM2 in this case. Further comparison of backscattering coefficient between the simulation, KA, and AIEM with $h = 1\,\text{cm}$, $l = 6\,\text{cm}$, $\theta = 40^\circ$ is shown

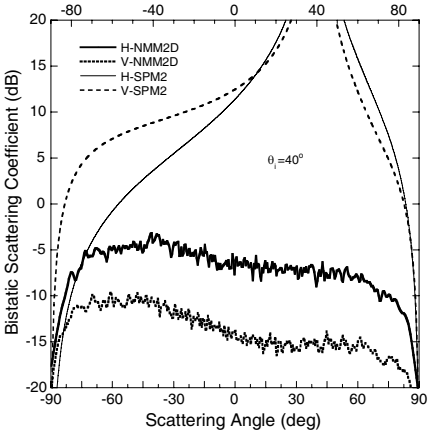

Figure 3. Comparison of bistatic scattering coefficients at 36.5 GHz between simulation (NMM2D) and the SPM2 model with $h = 2\,\text{cm}$, $l = 12\,\text{cm}$, $\theta = 40^\circ$. Both H (solid line) and V (dash line) polarizations are shown.

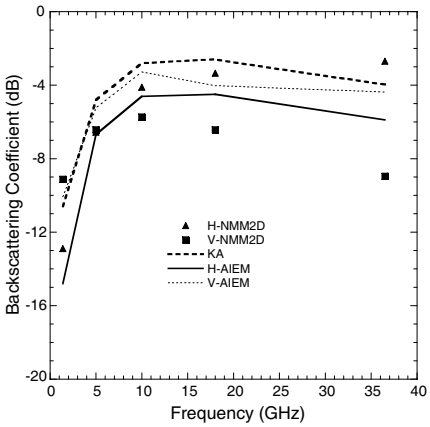

Figure 4. Comparison of backscattering coefficient between models: Kirchhoff Approximation (KA), AIEM and simulation (NMM2D) with $h = 1\,\text{cm}$, $l = 6\,\text{cm}$, $\theta = 40^\circ$. Simulation data are averaged over 40, 40, 50, 60, 60 realizations, respectively at 1.4 to 36.5 GHz.

in Fig. 4, where the simulation data were averaged over 40, 40, 50, 60, 60 realizations, respectively at 1.4 to 36.5 GHz, higher frequency with more realizations to get smoother curves. It is found that satisfactory prediction by AIEM is observed, but only up to C-band. At X-band and beyond, both emission models (KA and AIEM) gives different frequency trends with large level off. Fig. 5 presents comparison of emissivity between models and the simulation with $h = 1\,\text{cm}$, $l = 6\,\text{cm}$, $\theta = 40^\circ$. The SPM2 apparently fails to trace the frequency behavior at frequency beyond C-band. Compared to NMM2D, the KA always gives an underestimate and offers no polarization difference. While the AIEM and KA seem to trace the frequency trend quite well with NMM2D at H-polarized, they are largely level off at V-polarized, at which the AIEM underestimates the emission. It should be noted at this point that both the KA and AIEM used here only account for single scattering. The AIEM needs more complex computations to include the multiple scattering [16, 19]. Nevertheless, comparison showed here suggests that a significant multiple scattering occurs from the exponentially correlated surfaces. Even the surface remains the same with small slope, fine structures seems strongly responsible when frequency increases, implying the geometrical optic approach [4, 5] still not applicable.

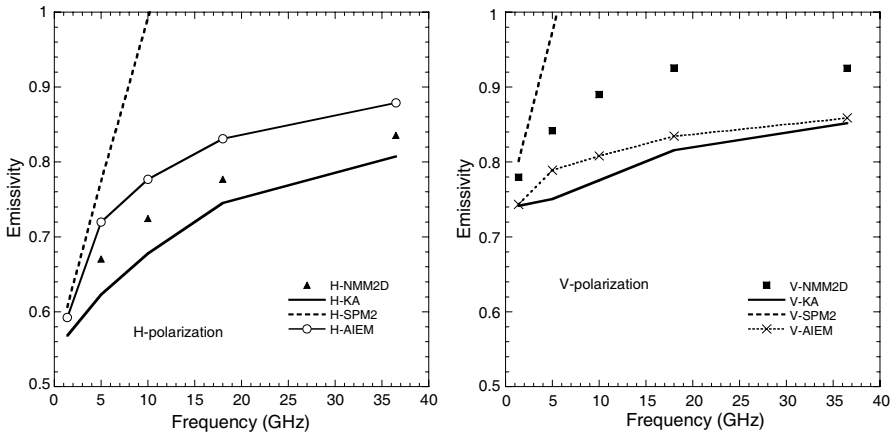

Figure 5. Comparison of emissivity between models (KA, SPM2, AIEM) and the simulation (NMM2D) with $h = 1\,\text{cm}$, $l = 6\,\text{cm}$, $\theta = 40^\circ$. Simulation data were averaged over 10 realizations. (a) For H-polarization. (b) For V-polarization.

3. RESULTS AND DISCUSSIONS

In this section we turn our focus on charactering the emission from the exponentially correlated surface by observing its frequency, polarization, and angular dependences. For reference, both the flat surface and the Gaussian correlated surface are presented. In all cases, the surface roughness parameters were chosen with $h = 1\,\text{cm}$, $l = 6\,\text{cm}$.

3.1. Frequency and Polarization Dependence

Figure 6 displays the H- and V-polarized emissivity from exponentially and Gaussian correlated surface covering a wide frequency bands of 1.4 GHz, 5 GHz, 10 GHz, 18 GHz, and 36.5 GHz. The emission from the Gaussian surface is relatively insensitive to frequency, particularly at V-polarized in which the frequency saturation seems occur very fast. On the contrary, emission from an exponential surface is more effective than that from the Gaussian one and increases with increasing frequency. To better observe the roughness effect, we plot the differences of emissivity between the rough and the flat surfaces as shown in Fig. 7. In all frequency bands under consideration, it clearly reveals that relatively small contributions were generated

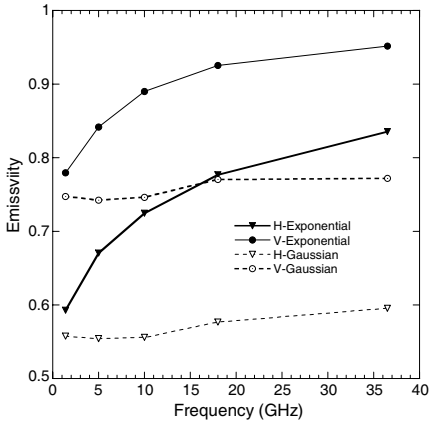

Figure 6. Comparison of emissivity between Gaussian (dashed line) and exponentially (solid line) correlated surfaces with $h = 1\,\text{cm}$, $l = 6\,\text{cm}$, $\theta = 40°$. Simulation data are averaged over 10 realizations.

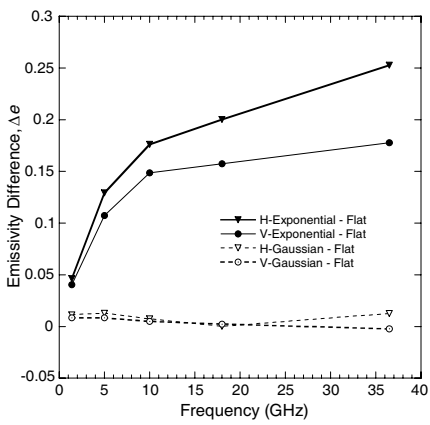

Figure 7. Emissivity difference between rough and flat surfaces for exponential and Gaussian correlation function with surface parameters same as in Fig. 6.

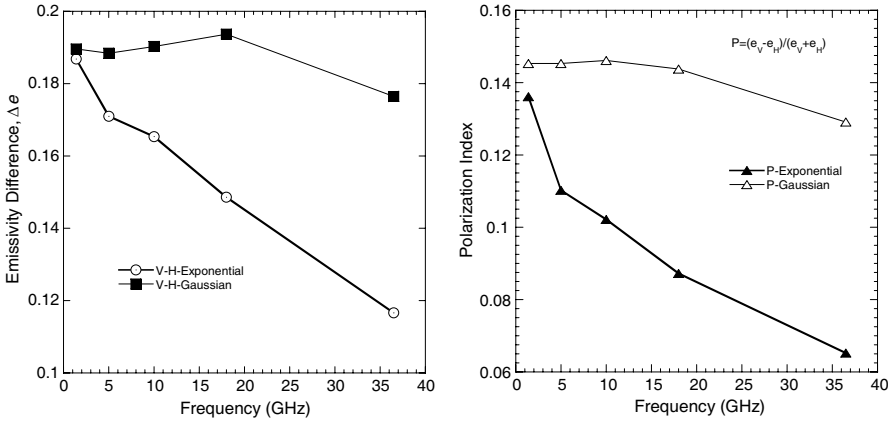

Figure 8. Polarization difference and polarization index of emissivity for Gaussian and exponential correlated surfaces with $h = 1\,\text{cm}$, $l = 6\,\text{cm}$, $\theta = 40^\circ$ as a function of frequency.

from Gaussian surfaces; even at 36.5 GHz, the polarization difference is almost negligible. Note that small fluctuations due to limited number of realizations are seen, but without affecting our observation and conclusion. As can be seen, the roughness contribution for an exponential surface, at L-band, is almost equal at both polarizations. It becomes more appreciable at C-band and beyond. At 36.5 GHz, the emissivity can be as large as 0.15 and 0.25 for V and H polarization, respectively. Comparatively, the surface roughness exercises more weightily on H-polarization through frequency changes. Hence, simply modifying Fresnel reflectivity by including the roughness parameter of the form $\exp[-4k^2h^2\cos^2\theta]$ fails to appropriately account for the roughness effects for exponential surfaces. Hence, in developing an empirical or semi-empirical emission models, the polarization dependence on the correlation function should be properly taken into account. The significant difference of emission, as compared to the flat surfaces, also suggests that the exponential surface bear much higher emission efficiency than the Gaussian surface. To further examine the roughness effect, in Fig. 8, we plot the polarization difference, $e_V - e_H$, and the polarization index, $(e_V - e_H)/(e_V + e_H)$ [6] as a function of frequency. It can be easily seen that for the Gaussian surface, both the polarization difference and index are less sensitive to frequency, compared to the exponential surface. Unlike the Gaussian surfaces, the polarization difference for the exponential surface decreases sharply with increasing frequency and the polarization index is even more

sensitive to frequency compared to polarization difference, revealing the distinct features of the emission behavior of the exponentially correlated surfaces.

3.2. Angular Behavior

In the above discussions, the look angle is fixed at 40°. It is useful to examine the angular behavior. To do so, we simulated the emissivity at 20, 30, 40, 50 and 60 degrees. For our purpose, only the exponential surface is considered. Fig. 9 shows the angular dependence as a function of frequency. Generally, H-polarized is more angle diverse than V-polarized emission, as expected from a small to moderate dielectric surfaces. For higher frequency, the V-polarized emission seems less angular sensitive. We now shall consider the polarization difference as a function of angle at various frequencies, as plotted in Fig. 10. A monotonically decrease of polarization difference with increasing frequency at larger look angle of 40–60 degrees is observed, while it quickly increases as frequency increases up to X-band and begins to decrease beyond that. Interesting to note is that at 40 degree, the frequency behavior of the polarization difference has less feature. At 18 GHz and beyond, the polarization difference looks quite linear as a function of look angle.

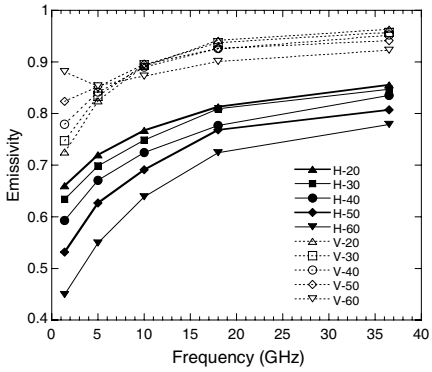

Figure 9. Comparison of emissivity for exponential correlated surfaces at look angles of 20, 30, 40, 50, and 60 degrees. Both H (solid lines) and V (dashed lines) polarizations are shown.

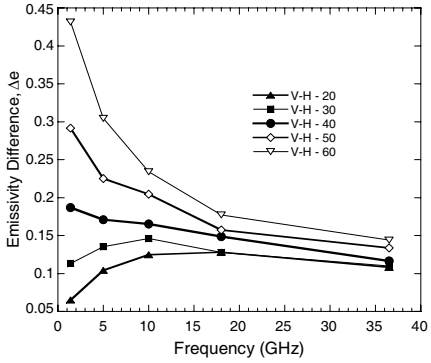

Figure 10. Polarization difference of the emissivity for the exponential correlated surfaces at look angles of 20, 30, 40, 50, and 60 degrees showing its dependence on angle.

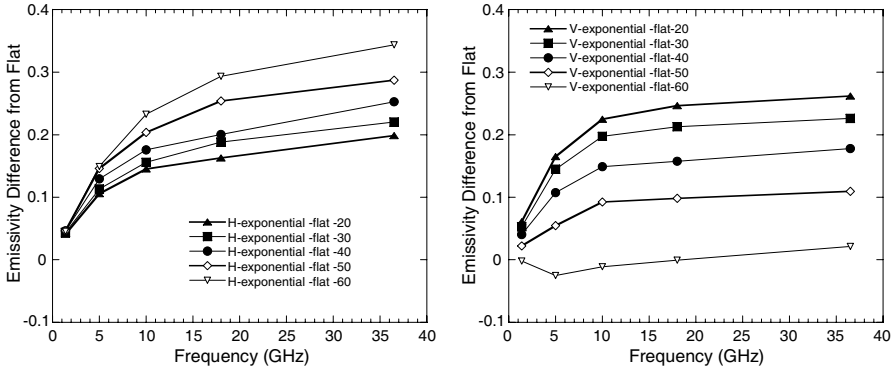

Figure 11. Emissivity difference between the exponential correlated and flat surfaces at look angles of 20, 30, 40, 50 and 60 degrees for both polarizations. (a) For H-polarization. (b) For V-polarization.

To further understand the angular behavior, the emissivity difference between the exponential surface and flat surface for H and V polarizations is presented in Fig. 11. Similar frequency trend at both polarizations is seen but in opposite direction, namely, when angle increases, the H-polarized emissivity difference increases but decreases for V-polarized. Some features need to bring out here. While the frequency trend is similar, the increasing rate is higher for H-polarized than V-polarized. At 60 degrees of look angle, the V-polarized emission from the exponential surface is even smaller than from the flat surface for frequency below 36.5 GHz.

3.3. Frequency Correlation

From above spectral analysis of the emission at various cases of rough surface, it is interesting to see the frequency correlation at L, C, X-bands. To do so, we conducted simulations from a pool of surface correlation length and *rms* height: l (cm) = {1.5, 3, 7, 6, 5, 9, 12, 15}, h (cm) = {0.25, 0.5, 1, 1, 1, 1.5, 2, 2.5}. For each case, 5 realizations were averaged over to obtain the simulated emissivity at look angle of 40 degrees. To illustrate the frequency correlation, we plot in Fig. 12, the emissivities of L band versus the emissivities of C band, and the emissivities of X band versus the emissivities of C-band. Correlation coefficients are then calculated. For C and L band, the correlation coefficients for both polarizations are quite closer to around 0.98; for C and X bands, the correlation for the H polarization is smaller than

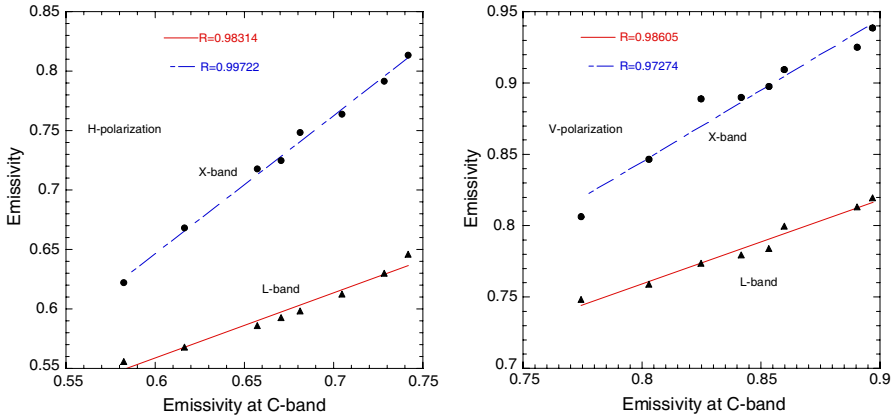

Figure 12. Frequency correlation of the emission for H (right) and V (left) polarizations at C-L and C-X bands. The solid and dash lines are linear regression fit with correlation coefficients indicated.

that for V polarization around 0.99 and 0.97, respectively. In general, results reveal that there is high correlation of emissivity at L-C and L-X bands. This is should be a useful indicator as long as the retrieval algorithm is concerned.

3.4. Effects on Soil Moisture Retrieval

Historically, the retrieval algorithm is to invert N unknown surface parameters to M observations or measurements, e.g., multi-frequency, multi-angular, multi-polarization. The algorithm is linear or, mostly, nonlinear, and is able to take system noise and uncertainties into account. Whatever it is linear or nonlinear, the relationship between surface parameters and emission measurements must correctly identified. From above sub-sections, charactering the emission from the exponentially correlated surface by observing its frequency, polarization, and angular dependences has been investigated. Unlike previously knowing that surface correlation plays little effects on emissivity, the following points for emission from exponentially correlated surface are noticed:

a. Surface roughness exercises more weightily on H-polarization through frequency changes. As a result, this phenomenon significantly affects on the relationship of the surface emission on the polarization ratio V/H measurements [11, 12].

b. Polarization difference decreases sharply with increasing frequency

and the polarization index is even more sensitive to frequency. It will result in estimation error when using both V- and H-polarization measurements if the surface roughness effects were assumed to be same in both polarizations as the current available semi-empirical or empirical model predictions [11, 12].

c. Generally, H-polarized exhibits more angle diverse than V-polarized emission, as expected from a small to moderate dielectric surfaces. For higher frequency, the V-polarized emission seems less angular sensitive. There is high correlation of emissivity at L-C and L-X bands.

By taking these facts into retrieval algorithm should be of interest to improve the accuracy and enhance sensitivity without introducing extra redundant or noisy signal.

4. CONCLUSIONS

In this paper, numerical simulations, NMM2D, were carried out to investigate the properties of the thermal emission from exponentially correlated surfaces by characterizing its spectral, angular, and polarization dependences. Very distinct emission behavior was observed between the exponential and Gaussian surfaces for which the former one has much higher emission efficiency due to its presence of fine scale structures that are captured by the NMM2D simulation results. The results presented in this study suggest that in retrieval of the soil moisture, the important role played by the exponential correlation function should be taken into account.

REFERENCES

1. Wang, J. R. and B. J. Choudhury, "Remote sensing of soil moisture content over bare fields at 1.4 GHz frequency," *J. Geophys. Res.*, Vol. 86, 5277–5282, 1981.
2. Tsang, L. and R. W. Newton, "Microwave emissions from soils with rough surfaces," *J. Geophy. Res.*, Vol. 87, No. 11, 9017–9024, 1982.
3. Wang, J. R. P. E. O'Neill, T. J. Jackson, and E. T. Engman, "Multi-frequency measurements of the effects of soil moisture, soil texture and surface roughness," *IEEE Transactions on Geoscience and Remote Sensing*, Vol. 21, 44–51, 1983.
4. Tsang, L., J. A. Kong, and R. T. Shin, *Theory of Microwave Remote Sensing*, John Wiley & Sons, 1985.

5. Ulaby, F. T., R. K. Moore, and A. K. Fung, *Microwave Remote Sensing*, Vol. 2, No. 3, Artech House, 1986.
6. Paloscia, S. and P. Pampaloni, "Microwave polarization index for monitoring vegetation growth," *IEEE Transactions on Geoscience and Remote Sensing*, Vol. 26, No. 5, 617–621, 1988.
7. Pampaloni, P. (ed.), *Microwave Radiometry and Remote Sensing Applications*, Brill Academic, Leiden, 1989.
8. Paloscia, S., P. Pampaloni, L. Chiarantini, P. Coppo, S. Gagliani, and G. Luzi, "Multifrequency passive microwave remote sensing of soil moisture and roughness," *Int. J. Remote Sensing*, Vol. 14, No. 3, 467–483, 1993.
9. Shi, J. C., J. Wang, A. Y. Hsu, P. E. O'Neill, and E. T. Engman, "Estimation of bare surface soil moisture and surface roughness parameter using L-band SAR image data," *IEEE Transactions on Geoscience and Remote Sensing*, Vol. 35, 1254–1266, Sep. 1997.
10. Njoku, E. G. and L. Li, "Retrieval of land surface parameters using passive microwave sensing at 6–18 GHz," *IEEE Transactions on Geoscience and Remote Sensing*, Vol. 37, No. 1, 79–93, 1999.
11. Shi, J., K. S. Chen, Q. Li, T. J. Jackson, P. E. O'Neill, and L. Tsang, "A parameterized surface reflectivity model and estimation of bare-surface soil moisture with L-band radiometer," *IEEE Transactions on Geoscience and Remote Sensing*, Vol. 40, No. 12, 2674–2686, 2002.
12. Shi, J. C., L. M. Jiang, L. X. Zhang, K. S. Chen, J.-P. Wigneron, and A. Chanzy, "A parameterized multifrequency-polarization surface emission model," *IEEE Transactions on Geoscience and Remote Sensing*, Vol. 43, No. 12, 2831–2841, 2005.
13. Fung, A. K., *Microwave Scattering and Emission Models and their Applications*, Artech House, 1992.
14. Chen, K. S., T. D. Wu, and J. C. Shi, "A model-based inversion of rough surface parameters from radar measurements," *Journal of Electromagnetic Waves and Applications*, Vol. 15, No. 2, 173–200, 2001.
15. Li, Q., J. C. Shi, and K. S. Chen, "A generalized power law spectrum and its applications to the backscattering of soil surfaces based on the integral equation model," *IEEE Transactions on Geoscience and Remote Sensing*, Vol. 40, No. 2, 271–281, 2002.
16. Chen, K. S., T. D. Wu, L. Tsang, Q. Li, and J. C. Shi, "Emission of rough surfaces calculated by the integral equation method with a comparison to a three-dimensional moment method simulations," *IEEE Transactions on Geoscience and Remote Sensing*, Vol. 41,

No. 1, 90–101, 2002.

17. Chen, K. S., A. K. Fung, J. C. Shi, and H.-W. Lee, "Intepretation of backscattering mechanism from non-gaussian correlated randomly rough surfaces," *Journal of Electromagnetic Waves and Applications*, Vol. 20, No. 1, 2233–2246, 2006.
18. Xu, P. and L. Tsang, "Bistatic scattering and emissivities of lossy dielectric surfaces with exponential correlation functions," *IEEE Transactions on Geoscience and Remote Sensing*, Vol. 45, No. 1, 62–72, 2007.
19. Fung, A. K. and K. S. Chen, *Microwace Scattering and Emission Models for Users*, Artech House, 2010.
20. Mattia, F., T. Le Toan, J. Souyris, G. Carolis, N. Floury, F. Posa, and G. Pasquariello, "The effect of surface roughness on multifrequency polarimetric SAR data," *IEEE Transactions on Geoscience and Remote Sensing*, Vol. 35, No. 4, 954–966, Jul. 1997.
21. Davidson, M. W. J., T. Le Toan, F. Mattia, C. Satalino, T. Manninen, and M. Borgeaud, "On the characterization of agricultural soil roughness for radar remote sensing studies," *IEEE Transactions on Geoscience and Remote Sensing*, Vol. 38, No. 2, 630–640, Mar. 2000.
22. Tsang, L., J. A. Kong, and K. H. Ding, *Scattering of Electromagnetic Waves: Theories and Applications*, Wiley, New York, 2000.
23. Tsang, L., D. Chen, P. Xu, Q. Li, and V. Jandhyala, "Wave scattering with the UV multilevel partitioning method: 1. Two-dimensional problem of perfect electric conductor surface scattering," *Radio Sci.*, Vol. 39, No. 5, 2004.
24. Xu, P. and L. Tsang, "Scattering by rough surface using a hybrid technique combining the multilevel UV method with the sparse matrix canonical grid method," *Radio Sci.*, Vol. 40, No. 4, 2005.
25. Hallikainen, M. T., F. T. Ulaby, M. C. Dobson, M. A. El-Rayes, and L. K. Wu, "Microwave dielectric behavior of wet soil — Part I: Empirical models and experimental observations," *IEEE Transactions on Geoscience and Remote Sensing*, Vol. 23, No. 1, 25–34, 1985.
26. Gu, X., L. Tsang, H. Braunisch, and P. Xu, "Modeling absorption of rough interface between dielectric and conductive medium," *Microw. Opt. Technol. Lett.*, Vol. 49, No. 1, 7–13, 2007.